Cellular and Molecular Life Sciences (2018) 75:2457–2471
https://doi.org/10.1007/s00018-017-2741-4

ORIGINAL ARTICLE

Molecular function of the novel α7β2 nicotinic receptor

Beatriz E. Nielsen[1] · Teresa Minguez[2] · Isabel Bermudez[2] · Cecilia Bouzat[1]

Received: 18 September 2017 / Revised: 30 November 2017 / Accepted: 27 December 2017 / Published online: 8 January 2018

Abstract

The α7 nicotinic receptor is a promising drug target for neurological and inflammatory disorders. Although it is the homomeric member of the family, a novel α7β2 heteromeric receptor has been discovered. To decipher the functional contribution of the β2 subunit, we generated heteromeric receptors with fixed stoichiometry by two different approaches comprising concatenated and unlinked subunits. Receptors containing up to three β2 subunits are functional. As the number of β2 subunits increases in the pentameric arrangement, the durations of channel openings and activation episodes increase progressively probably due to decreased desensitization. The prolonged activation episodes conform the kinetic signature of α7β2 and may have an impact on neuronal excitability. For activation of α7β2 receptors, an α7/α7 binding-site interface is required, thus indicating that the three β2 subunits are located consecutively in the pentameric arrangement. α7-positive allosteric modulators (PAMs) are emerging as novel therapeutic drugs. The presence of β2 in the pentamer affects neither type II PAM potentiation nor activation by an allosteric agonist whereas it impairs type I PAM potentiation. This first single-channel study provides fundamental basis required to decipher the role and function of the novel α7β2 receptor and opens doors to develop selective therapeutic drugs.

Keywords Cys-loop receptors · Nicotinic receptor · Single-channel recordings · Patch-clamp

Abbreviations

nAChR	Nicotinic acetylcholine receptor
ACh	Acetylcholine
PAM	Positive allosteric modulator
5-HI	5-Hydroxyindole
α7LC	α7 low conductance
TM	Transmembrane domain

Introduction

The α7 nicotinic acetylcholine receptor (nAChR) is one of the most abundant nAChRs in the brain. It is especially located in the hippocampus, thalamus, and cortex and contributes to cognition, attention, and working memory [1–3]. Decline or alterations of cholinergic signaling involving α7 have been implicated in neurological diseases, such as schizophrenia, epilepsy and Alzheimer disease [1, 4]. α7 is also expressed in non-neuronal cells where it plays a role in immunity, inflammation and neuroprotection [4, 5]. Enhancement of α7 activity is emerging as a potential therapeutic treatment for neurological, psychiatric, and inflammatory disorders [2–4, 6–9]. In particular, positive allosteric modulators (PAMs), which act only in the presence of the endogenous agonist, are emerging as novel tools to enhance α7 function [2, 3, 7, 10, 11]. Allosteric ligands have several advantages, including higher receptor subtype selectivity and conservation of the spatial and temporal pattern of activation by the endogenous neurotransmitter [7]. α7 PAMs are classified as type I and type II based on their effects on macroscopic currents. Both types of α7 PAMs increase receptor sensitivity to agonists, current magnitudes, and empirical Hill coefficients. The type I PAMs (for example, 5-HI or NS-1738) do so with little or no effect on the onset and decay rates of the macroscopic responses to the agonist, while the type II PAMs (for example PNU-120596) markedly slow current decay rate and can also reactivate desensitized receptors [6, 10–13].

✉ Cecilia Bouzat
inbouzat@criba.edu.ar

[1] Instituto de Investigaciones Bioquímicas de Bahía Blanca, Departamento de Biología, Bioquímica y Farmacia, Universidad Nacional del Sur-Consejo Nacional de Investigaciones Científicas y Técnicas (UNS-CONICET), 8000 Bahía Blanca, Argentina

[2] Department of Medical and Biological Sciences, Oxford Brookes University, Oxford OX3 0BP, UK

α7 was classically considered to be the homomeric member of the family. However, recent evidence has demonstrated the presence of heteromeric α7β2 nAChR in rodent and human brain [14–17]. The physiological role of this receptor is not yet known, but it might be involved in therapeutic and pathological processes, such as anesthesia and Alzheimer's disease [14, 15, 18, 19].

To date, the determination of functional properties of α7β2 receptors has been restricted to the macroscopic level [14–18, 20, 21]. Currents from the heteromeric receptors have been recorded from neurons [14, 15, 18] and from heterologous expressing systems using unlinked subunits [17, 18, 20, 21] or concatenated α7 with one or two β2 subunits [16].

Whether α7β2 exhibits an altered pharmacological and functional profile compared to α7 is still unclear (reviewed in [22]). To find a way to unequivocally establish the functional signature of α7β2, we used two different approaches combined with patch-clamp recording to monitor single-channel properties of receptors with defined stoichiometry. One strategy is based on the concatemeric technology, which allows control of stoichiometry and limits expression to exactly one receptor subtype [3, 23–25]. To confirm the functional equivalence of the concatemeric with the wild-type receptor [26], we also applied the electrical fingerprinting strategy with unlinked subunits [3, 27–30]. To this end, we used an α7 subunit carrying a triple mutation at the intracellular region as a reporter of subunit stoichiometry (α7LC for low conductance). Homomeric α7LC receptors are functional but single-channel openings cannot be detected due to their low amplitude. Co-expression of α7LC with α7 leads to multiple and discrete amplitude classes, each corresponding to receptors of a given stoichiometry [27–31]. In an analogous manner, we here combined α7LC with β2, and inferred the possible stoichiometries of functional heteromeric receptors through the detected amplitude classes.

Our results, which include the first report of single α7β2 channels, reveal the possible heteromeric arrangements, the contribution of β2 subunit to channel kinetics and ion channel conductance, and the differences on PAM selectivity with α7. This information could be useful for identifying functional heteromeric receptors in native cells and for understanding their distinct roles; and opens doors for the development of specific ligands.

Materials and methods

Drugs

Acetylcholine (ACh) and 5-hydroxyindole (5-HI) were purchased from Sigma-Aldrich (St. Louis, MO, USA). PNU-120596 (*N*-(5-chloro-2,4-dimethoxyphenyl)-*N*′-(5-methyl-3-isoxazolyl)-urea) and 4BP-TQS (4-(4-bromophenyl)-3a,4,5,9b-tetrahydro-3H-cyclopenta[c]quinoline-8-sulfonamide) were obtained from Tocris Biosciences (Bristol, UK). NS-1738 (*N*-(5-chloro-2-hydroxyphenyl)-*N*′-[2-chloro-5-(trifluoromethyl)phenyl]urea) was purchased from Santa Cruz Biotechnology (Dallas, TX, USA).

Site-directed mutagenesis

Human α7 and β2 subunits were used. Mutations were generated using the QuikChange® Site-Directed Mutagenesis kit (Agilent, UK). The low conductance form of α7 (α7LC) contained three mutations at the intracellular loop (Q428R, E432R, S436R [29]).

Construction of pentameric concatemers

Concatenated subunit receptors were constructed as described before for α4β2 receptors [23–25, 32]. Briefly, two consecutive PCR steps were used to prepare the subunits for concatenation. The first PCR step eliminated stop codons (for all constructs) and inserted the kozac sequence GCCACC immediately before the signal peptide of the first subunit. Half of the length of the linkers was added with the first PCR step upstream and downstream from the 5′ and 3′ coding regions of each subunit. The second PCR step introduced unique restriction sites upstream and downstream of the linkers to allow successive subcloning into a modified pcDNA3.1 hygro (−) plasmid vector (Invitrogen, UK). This plasmid was also used to assemble the concatemers. To facilitate assembly and subcloning, *Asc*I, *Xba*I and *Age*I restriction sites were inserted by oligonucleotide hybridization between the *Nhe*I and *Xho*I sites in the multiple cloning site of the plasmid. For all constructs, the enzyme restriction sites introduced were: 1st subunit *Asc*I/*Xba*I; 2nd subunit *Xba*I/*Age*I; 3rd subunit *Age*I/*Xho*I; 4th subunit *Xho*I/*Not*I; 5th subunit *Not*I/*Eco*RV.

The signal peptide was removed from all the subunits except in the first and the subunits were bridged by tripeptide alanine–glycine–serine linkers (AGS) of variable length to compensate differences in the length of the C-terminus of the α7 and β2 subunits. The number of the AGS repeats was 10 for α7–α7, 9 for α7–β2, and 8 for β2–α7. The total number of residues from the C-terminal domain to the N-terminal domain of the following subunit was 44 (α7–α7), 41 (α7–β2), and 48 (β2–α7). Following assembly, pentameric concatamers were subcloned into the vector pCI (Promega, UK). The presence of a pentameric concatenated construct was verified by enzymatic digestion (*Eco*RV, *Xho*I) taking advantage of the restriction sites between subunits followed by electrophoresis in agarose gel (0.8%) to detect

the fragments with specific lengths. Concatemeric receptors were first tested by functional assays in oocytes.

To engineer α7β2 nAChR containing β2 L9′T subunits, L9′T mutation was first introduced into the desired β2 subunit subcloned into the modified pCI vector. The mutated subunit was then ligated into the concatemer using unique restriction enzyme sites. To confirm that the mutated subunit was incorporated into the concatemer, the subunit was cut from the concatemer using unique restriction enzyme sites and then its nucleotide sequence was verified by DNA sequencing (SourceBioscience, UK, Eurofins, UK). All concatemeric constructs were assayed for integrity using restriction enzyme digestion.

Expression of receptors in mammalian cells

Receptors were transiently expressed in BOSC 23 cells, which are modified HEK 293T cells (provided by Dr. Sine, Mayo Clinic, USA). The cells were tested to discard mycoplasma contamination by 4,6-diamidino-2-phenylindole (DAPI) staining and fluorescent microscopy. Cells were transfected by calcium phosphate precipitation with subunit or concatemeric cDNAs together with Ric-3 and/or NACHO cDNAs for cell surface expression [29, 33]. GFP cDNA (5% of total cDNA amount) was incorporated during the transfection to allow identification of transfected cells. The ratio for unlinked subunit cDNAs was α7:β2 1:8 or 1:10, and the ratio for nAChR subunit and chaperone (Ric-3 or NACHO) cDNA was 1:4. For concatemers, the ratio was concatemer: Ric-3 1:4 or concatemer: Ric-3: NACHO 1:1:1. We did not observe significant differences in the expression among these conditions. All transfections were carried out for about 8–12 h in DMEM with 10% FBS and were terminated by exchanging the medium. Cells were used for single-channel recordings 2–3 days after transfection at which the maximum expression levels are usually achieved [29–31, 33–36].

Single-channel recordings

Single-channel recordings were obtained in the cell-attached patch configuration [33]. Each patch corresponds to a different cell (*n* indicates the number of independent experiments). For each condition (different receptors or drugs), at least three different cell transfections from different days were used for the recordings.

The bath and pipette solutions contained 142 mM KCl, 5.4 mM NaCl, 1.8 mM $CaCl_2$, 1.7 mM $MgCl_2$ and 10 mM HEPES (pH 7.4). For potentiation, 2 mM 5-HI, 10 μM NS-1738 or 1 μM PNU-120596 was added to the pipette solution with ACh. Thus, single channels were recorded in the continuous presence of the drugs. Typical recordings lasted between 5 and 10 min. The final concentration of DMSO used to solubilize PAMs (PNU-120596 and NS-1738) was lower than 0.1% (v/v). This DMSO concentration does not affect α7 activation properties [29, 36]. ACh and 5-HI were solubilized directly in pipette solution [29]. For recordings in the absence of calcium, the pipette solution contained 80 mM KF, 20 mM KCl, 40 mM K-aspartate, 2 mM $MgCl_2$, 1 mM EGTA and 10 mM HEPES (pH 7.4) [30]. Single-channel currents were digitized at 5–10 μs intervals, low-pass filtered at a cut-off frequency of 10 kHz using an Axopatch 200B patch-clamp amplifier (Molecular Devices Corp., CA) and analyzed using the program TAC (Bruxton Corporation, Seattle, WA, USA) with the Gaussian digital filter at 9 kHz (Final cut-off frequency 6.7 kHz). In the presence of PNU-120596 or 4BP-TQS, the filter was 3 kHz as described before [29, 37]. Open time histograms were fitted by the sum of exponential functions by maximum likelihood using the program TACFit (Bruxton Corporation, Seattle, WA, USA). Bursts of channel openings were identified as a series of closely separated openings preceded and followed by closings longer than a critical duration, which was taken as the point of intersection between components as described before [29, 33].

Critical durations were defined by the intersection between the first and second briefest components in the closed-time histogram for bursts of α7, $(\alpha7)_5$ and $(\alpha7)_4\beta2$ (~ 200–400 μs) and second and third closed components for bursts of $(\alpha7)_3(\beta2)_2$ and $(\alpha7)_2(\beta2)_3$ (~ 2–6 ms), in the absence of PAMs.

In the presence of potentiators, the critical time was defined for α7 and different concatemeric receptors between the second and third closed components in presence of 5-HI (~ 2–6 ms), between the third and fourth closed components in the presence of NS-1738 (~ 10–20 ms) and between the third and fourth closed components in the presence of PNU-120596 (~ 60–100 ms). The longest duration closed components were not considered for the analysis since they vary with the expression level of α7 in each cell.

Electrical fingerprinting strategy

To define amplitude classes from receptors generated by co-expression of high and low conductance subunits, analysis was performed by tracking events regardless of current amplitude. Amplitude histograms were then constructed, and the different amplitude classes were distinguished. Open time histograms were then constructed for a given amplitude class by selecting only openings with amplitudes of ± SD pA of that of the mean of the class [27–29].

Expression and electrophysiology in *Xenopus* oocytes

Stage V and VI *Xenopus* oocytes were prepared as previously described [24], and then injected with 100 ng of α7,

$(\alpha7)_5$ or concatemeric α7β2 receptor cRNA. Injected oocytes were incubated until use at 18 °C in Barth's solution: 88 mM NaCl, 1 mM KCl, 0.33 mM $Ca(NO_3)_2$, 0.41 mM $CaCl_2$, 0.82 mM $MgSO_4$, 2.4 mM $NaHCO_3$, and 10 mM HEPES, supplemented with 0.1 mg/mL streptomycin, 1000 U/mL penicillin and 100 µg/mL amikacin (pH 7.5, with 5 M NaOH).

Oocytes were impaled by two microelectrodes filled with 3 M KCl (0.5–2.0 MΩ) and voltage-clamped at − 60 mV using an Oocyte Clamp OC-725C amplifier (Warner Instruments, USA) and Labscribe software (Iworx, NH, USA). All experiments were carried out at room temperature. ACh concentration–response curves were obtained by normalizing ACh-induced responses to the control responses induced by 1 mM ACh in the same oocyte (a near-maximum effective concentration at α7 as well as α7β2 receptors). An interval of 5 min was allowed between agonist applications, as this was found to be sufficient to ensure reproducible recordings. Allosteric modulators (PNU-120596 or 5-HI) were co-applied with ACh EC_{20} (30 µM) for the receptor under study and the peak current responses were normalized to the responses elicited by ACh EC_{20} alone in the same oocyte.

Concentration–response curves for ACh or allosteric modulators were fitted by a nonlinear least-squares algorithm according to the equation: $I = I_{max}/[1 + (EC50/x)n]$, in which I_{max} is the maximum obtainable peak current; EC_{50} is the concentration of the agonist that elicits 50% of the maximum obtainable peak current; x is the agonist or allosteric modulator concentration and n is the slope factor.

Statistical analysis

Data were presented as mean ± SD, or as mean ± SEM only when indicated. Data sets that passed the Shapiro–Wilk test for normality and the Levene median test for equal variance were analyzed using two-tailed Student's t test for pairwise comparisons or oneway ANOVA followed by Bonferroni's post hoc tests for multiple comparisons. All the tests were performed with SigmaPlot 12.0 (Systat Software, Inc.). Statistically significance difference was established at p values < 0.05 ($p < 0.05$*, $p < 0.01$**, $p < 0.001$***). Concentration–response curves were determined by nonlinear regression fits to the Hill equation using Prism 5.0 (GraphPad, San Diego, CA).

Results

α7 concatemeric receptors

The α7 concatemeric receptor, $(\alpha7)_5$, was constructed by linking five human α7 subunits (Fig. 1a), expressed in BOSC 23 cells, and examined by single-channel recording.

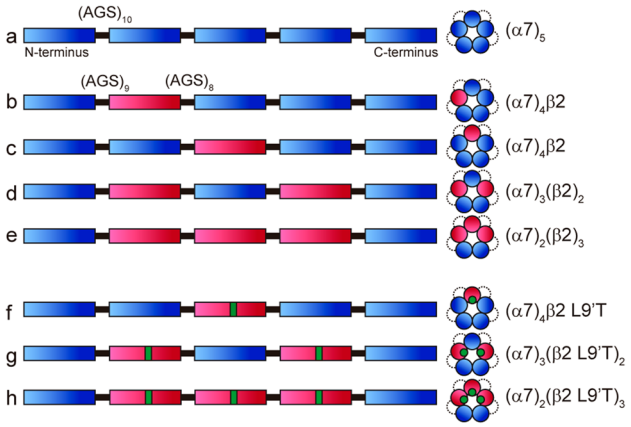

Fig. 1 Schematic diagram of pentameric concatenated constructs. α7 and β2 subunits are shown in blue and red, respectively. Subunits containing TM2 L9′T mutation are shown in green. The linkers of AGS are represented with black lines in linear constructs and dotted lines bridging the subunits in the assembled concatemers

In the presence of 100–500 µM ACh, α7 exhibits infrequent and single brief openings (~ 0.25 ms) flanked by long closings, or less often, several openings in quick succession, known as bursts (Fig. 2a, Table 1, [29, 33]). Discarding the lower frequency of channel openings, there are no statistically significant differences in mean open and burst durations of $(\alpha7)_5$ ($n = 3$) respect to wild-type α7 ($n = 4$) ($p > 0.05$, Fig. 2a, Table 1). For both receptors, channels show a broad amplitude distribution due to the lack of resolution of the brief events, being the maximal amplitude of ~ 10 pA at − 70 mV (Fig. 2a, [33]).

No single-channel activity elicited by ACh was detected from non-transfected cells ($n = 8$) or from cells transfected only with Ric-3 cDNA ($n = 7$) or Ric-3: NACHO (1:1) ($n = 5$). Also, channel activity was not detected from transfected cells in the absence of ACh ($n = 5$).

For both α7 and $(\alpha7)_5$ receptors, 100 µM ACh in the presence of the type II PAM PNU-120596 elicits significantly prolonged openings of ~ 10 pA (− 70 mV). Openings separated by brief closings are grouped in bursts, which in turn coalesce into long activation periods, named clusters (~ 1–3 s) (Table 1, Fig. 2b, [35, 36]). The mean duration of the slowest open component and the mean cluster duration of potentiated $(\alpha7)_5$ ($n = 3$) are indistinguishable from those of wild-type α7 ($n = 8$) ($p > 0.05$, Fig. 2b, Table 1).

In agreement with the single-channel results, the EC_{50} values for ACh as well as for two different types of PAMs, PNU-120596 (type II PAM) and 5-HI (type I PAM), determined from macroscopic currents in oocytes, are identical between α7 ($n = 10$) and $(\alpha7)_5$ ($n = 10$) ($p > 0.05$, Fig. 3a–c, Table 2).

These findings led us to conclude that the concatemeric receptor $(\alpha7)_5$ has comparable pharmacological signatures,

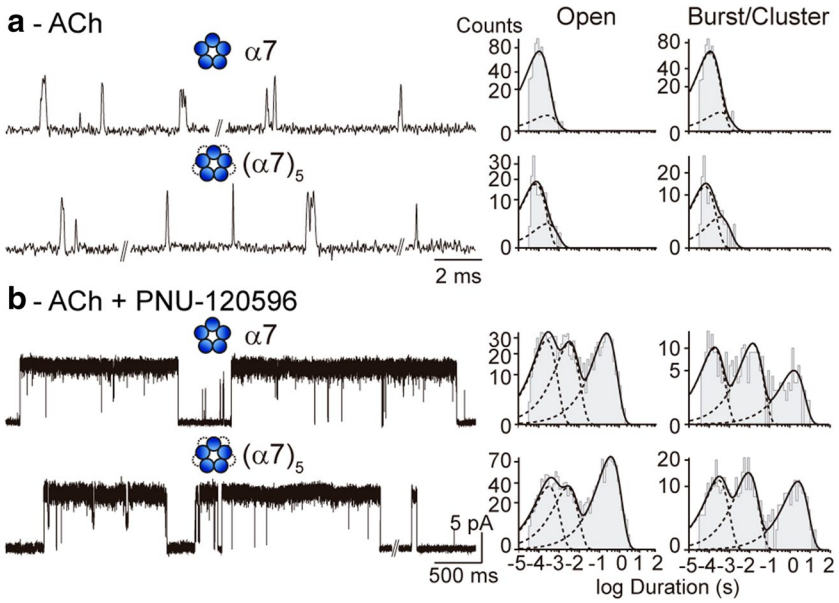

Fig. 2 Comparison between single-channel profiles of α7 and $(α7)_5$. Left: typical single-channel traces from recordings in the continuous presence of 100 μM–1 mM ACh (**a**) or 100 μM ACh + 1 μM PNU-120596 (**b**). Right: typical open and burst/cluster duration histograms are shown. Channel openings are shown as upward deflections. Membrane potential: − 70 mV. Filter: 9 kHz (**a**) and 3 kHz (**b**)

Table 1 Mean open and burst or cluster durations of α7 and α7β2 concatemeric receptors in the absence or presence of PAMs

Receptor	Agonist	PAM	τ_{open} (ms)	τ_{burst} or $\tau_{cluster}$ (ms)	*n*
α7	100 μM–1 mM ACh	–	0.25 ± 0.01	0.34 ± 0.01	4
α7	100 μM ACh	1 μM PNU-120596	221 ± 72***	1988 ± 718***	8
α7	500 μM ACh	2 mM 5-HI	2.26 ± 0.33***	5.20 ± 0.28***	4
α7	500 μM ACh	10 μM NS-1738	2.91 ± 0.66*	18.42 ± 3.00***	4
$(α7)_5$	100 μM–1 mM ACh	–	0.24 ± 0.02	0.33 ± 0.02	3
$(α7)_5$	100 μM ACh	1 μM PNU-120596	205 ± 44***	1867 ± 937***	3
$(α7)_4β2$	100 μM–1 mM ACh	–	0.22 ± 0.10	0.49 ± 0.02	3
$(α7)_4β2$	100 μM ACh	1 μM PNU-120596	256 ± 79**	2229 ± 442***	5
$(α7)_4β2$	500 μM ACh	2 mM 5-HI	1.64 ± 0.64**	6.24 ± 0.86***	4
$(α7)_3(β2)_2$	100 μM–1 mM ACh	–	0.41 ± 0.03	0.98 ± 0.02	3
$(α7)_3(β2)_2$	100 μM ACh	1 μM PNU-120596	234 ± 57***	2382 ± 540***	5
$(α7)_3(β2)_2$	500 μM ACh	2 mM 5-HI	0.93 ± 0.14**	4.14 ± 0.10***	4
$(α7)_2(β2)_3$	100 μM–1 mM ACh	–	0.52 ± 0.06	2.42 ± 0.79	5
$(α7)_2(β2)_3$	100 μM ACh	1 μM PNU-120596	178 ± 45***	2081 ± 587***	4
$(α7)_2(β2)_3$	500 μM ACh	2 mM 5-HI	0.74 ± 0.01***	2.54 ± 0.20	4
$(α7)_2(β2)_3$	500 μM ACh	10 μM NS-1738	2.28 ± 0.57***	10.46 ± 3.22***	5

τ_{open} and τ_{burst} or $\tau_{cluster}$ correspond to the slowest open components of the corresponding histograms. Single-channel currents were recorded in the continuous presence of agonist alone or combined with PAMs. Values are mean ± SD. *n*: number of independent experiments, each from different cell patches. Statistical significance was determined by comparing the mean value in the presence of the PAM respect to the absence of the PAM by two-tailed Student's *t* test ($p < 0.05$*, $p < 0.01$**, $p < 0.001$***)

in terms of activation by its endogenous agonist and potentiation by two types of PAMs, to those of wild-type α7 receptors. It is an important control that shows that concatenation of α7 subunits does not affect the functional properties of the receptor, and therefore, concatemeric receptors are valid models of wild-type receptors. Therefore, we next constructed concatemers combining α7 and β2 subunits in different stoichiometries to be used as models of native α7β2 receptors.

Kinetic signature of α7β2 concatemeric receptors

To determine how the number of β2 subunits contributes to function, we constructed concatemeric receptors containing one, two or three β2 subunits (Fig. 1b–e). All concatemeric receptors are functional in oocytes, and their EC_{50} values for ACh are similar to that of α7 ($p > 0.05$, $n = 6$–10 for each receptor, Fig. 3a and Table 2).

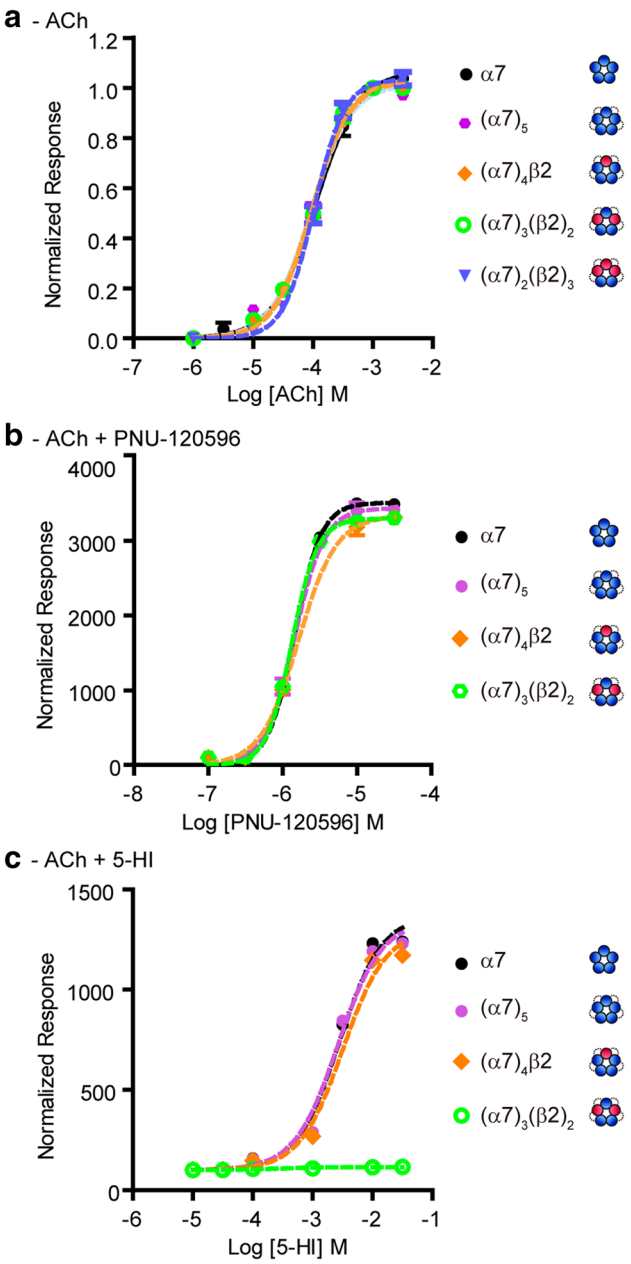

Fig. 3 Pharmacological properties of human α7, $(α7)_5$ and α7β2 concatameric receptors expressed in *Xenopus* oocytes. Concentration-dependent effects of ACh (**a**), PNU-120596 (**b**) or 5-HI (**c**) were fitted by the Hill equation, as described in "Materials and methods". Dose–response curves were obtained from macroscopic currents elicited by ACh at different concentrations (**a**), or by 30 μM ACh, which corresponds to the EC_{20} value, in the presence of different concentrations of the PAMS (**b**, **c**). Data points are mean values ± SEM of α7 (n = 10), $(α7)_5$ (n = 10), $(α7)_4β_2$ (n = 8), $(α7)_3(β2)_2$ (n = 8) and $(α7)_2(β2)_3$ (n = 6). n corresponds to the number of independent experiments (oocytes) for each condition. EC_{50} and percentage of maximal potentiation values are shown in Table 2

When expressed in BOSC 23 cells, ACh-elicited single-channel currents of receptors comprising one β2 subunit in the second position of the linear sequence $(α7)_4β2$ show a maximal mean amplitude of ~ 10 pA, similar to that of α7 (Figs. 1b, 4b). The presence of one β2 subunit does not change significantly open channel lifetime ($p > 0.05$, $n = 3$). However, the burst duration increases ~ 1.5-fold with respect to α7 ($p < 0.001$, $n = 3$, Table 1, Fig. 4b).

Changing the position of the β2 subunit in the linear arrangement from the second to the third place (Fig. 1c) leads to channels with identical burst and open durations as those of $(α7)_4β2$ with β2 in the second position (Fig. 4b).

Concatemeric receptors with two alternate β2 subunits are also functional (Fig. 1d). The second β2 subunit leads to an additional increase in mean open and burst durations, which are ~ 1.6-fold ($p < 0.01$, $n = 3$) and ~ threefold ($p < 0.001$, $n = 3$), respectively, longer than those of α7 (Table 1, Fig. 4c). The maximal amplitude remains constant (~ 10 pA). Another construct containing two alternate β2 subunits but starting with β2 in the linear sequence did not show functional expression in BOSC 23 cells.

A pentameric arrangement with three consecutive β2 subunits $(α7)_2(β2)_3$ (Fig. 1e) also forms functional channels. For this arrangement, open channel lifetime and burst durations are even more prolonged than in $(α7)_3(β2)_2$ receptors, and are twofold ($p < 0.001$, $n = 5$) and sevenfold ($p < 0.05$, $n = 5$) longer with respect to α7 (Table 1, Fig. 4d). Again, single-channel amplitude remains constant with respect to α7.

Thus, the increase in the number of β2 subunits leads to a linear increase in the open channel lifetime (Fig. 5a). From the slope of the curve, we determined that each β2 subunit contributes to 0.10 ± 0.03 ms. Interestingly, the burst duration increases exponentially with the number of β2 subunits, indicating that it is more sensitive to the presence of this subunit (inset to Fig. 5a).

The amplitude histograms constructed only for events longer than 0.3 ms to allow full amplitude resolution show no statistically significant differences ($p > 0.05$) between α7 (9.65 ± 0.41 pA, $n = 4$) and $(α7)_2(β2)_3$ (9.70 ± 0.21 pA, $n = 3$) (Fig. 5b).

α7β2 concatemeric receptors carrying pore-lining mutations

The ring of hydrophobic residues in TM2 at 9′ position forms the channel gate [38]. Replacement by polar residues significantly increases open probability [20, 39]. As another means to confirm the assembly of β2 with α7 and to determine the functional contribution of the hydrophobic residues at TM2 9′, we incorporated the L9′T mutation in the β2 subunit of the concatemeric receptors and compared channel activity of the mutant heteromeric receptors with that of α7L9′T receptors. The single-channel pattern of α7L9′T shows, instead of the typical isolated brief openings of α7 wild-type receptors, long-duration bursts (~ 200 ms), and,

Table 2 Concentration effects of ACh, PNU-120596 and 5-HI on α7, $(α7)_5$ and α7β2 concatemeric receptors

Receptor	ACh	PNU-120596		5-HI		*n*	*N*
	EC_{50} (μM)	EC_{50} (μM)	% potentiation	EC_{50} (mM)	% potentiation		
α7	108 ± 5	1.5 ± 0.2	3513 ± 33	2.8 ± 0.6	1376 ± 105	10	5
$(α7)_5$	93 ± 5	1.5 ± 0.4	3492 ± 85	2.6 ± 0.3	1346 ± 205	10	5
$(α7)_4β2$	95 ± 4	1.6 ± 0.2	3338 ± 76	3.2 ± 0.8	1301 ± 114	8	5
$(α7)_3(β2)_2$	97 ± 6	1.4 ± 0.3	3300 ± 50	2.4 ± 0.6	114 ± 6***	8	5
$(α7)_2(β2)_3$	104 ± 12	ND	ND	ND	ND	6	5

The concentration-dependent effects of PNU-120569 or 5-HI were determined on ACh responses elicited by EC_{20} ACh (30 μM). The data points were used to generate concentration response curves from which EC_{50} was estimated, as described in "Materials and methods". The percentage of maximal potentiation was calculated as $(I_{ACh\ EC20+PAM})/I_{ACh\ EC20}$. Values represent the mean ± SEM. Statistical analysis on ACh and PAMs was conducted using oneway ANOVA followed by Bonferroni's post hoc tests for multiple comparisons ($p < 0.05$*, $p < 0.01$**, $p < 0.001$***, ND: not determined). *N* is the number of batches of oocytes used for experiments and n corresponds to the number of independent experiments carried out

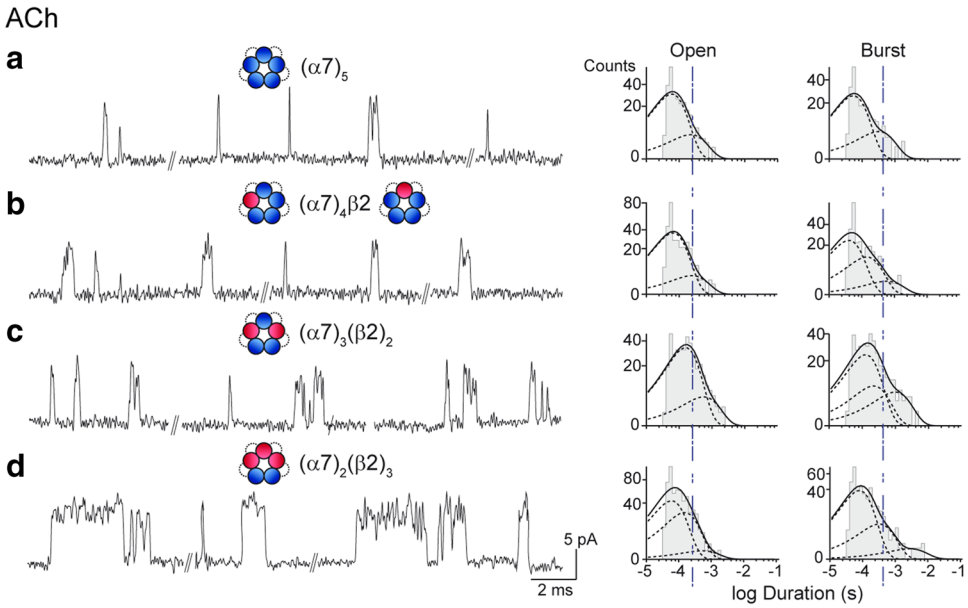

Fig. 4 Kinetic properties of concatemeric receptors with increasing number of β2 subunits. Left: typical traces from single-channel recordings of concatemeric receptors in the continuous presence of 1 mM ACh. Right: representative open and burst duration histograms. Blue dotted lines indicate the mean open and burst durations for $(α7)_5$ showing their increase with the increase in the number of β2 subunits. Membrane potential: − 70 mV. Filter: 9 kHz. Channel openings are shown as upward deflections

occasionally, super long-duration clusters (~ 1 s) containing openings of ~ 10 ms (Fig. 6a). The activity patterns of concatemeric receptors containing wild-type α7 together with one, two or three β2 subunits carrying the L9′T mutation (Fig. 1f–h) are also strikingly different from their respective controls (Fig. 6). For receptors with one mutant β2 subunit, open channel lifetime (0.61 ± 0.06 ms, $n = 5$) and mean burst duration (3.31 ± 1.22 ms, $n = 5$) are longer than the corresponding control. Occasionally, even longer openings (~ 3–4 ms) forming clusters of ~ 100–200 ms are detected (Fig. 6b). Activity patterns of concatemeric receptors with two and three mutant β2 subunits exhibit a similar variable behavior but even more prolonged openings and bursts respect to their controls (Fig. 6c–d). Receptors with three β2L9′T subunits show several long-duration open components (0.72 ± 0.04, 2.28 ± 0.20, 8.28 ± 2.00 ms, $n = 4$). Occasionally, very long-duration clusters (1459 ± 156 ms) containing even more prolonged openings (43.90 ± 7.40 ms) are observed (Fig. 6d). Thus, we conclude that β2 is incorporated into the pentamer and contributes to channel gating and to the stability of the open channel.

Positive allosteric modulation of α7β2 concatemeric receptors

PAMs have been developed as selective allosteric ligands for α7 homomeric receptors. However, the presence of α7β2 heteromeric receptors led us to explore if PAMs can also act at α7β2 instead of being selective for α7. To determine the effects of α7 PAMs on α7β2 receptors, single-channel currents elicited by ACh in the presence of either type II PAMs (PNU-120596) or type I PAMs (5-HI or NS-1738) were recorded.

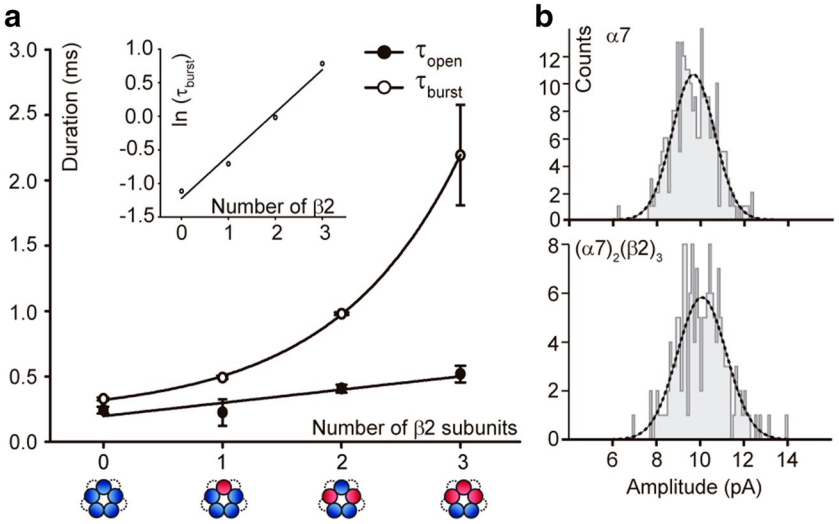

Fig. 5 Single-channel properties of α7β2 concatemeric receptors. **a** Plot of mean open (τ_{open}) and burst (τ_{burst}) durations as a function of the number of β2 subunits in the receptor. Data are plotted as mean ± SEM for zero β2 ($n = 3$), one β2 ($n = 3$), two β2 ($n = 3$) and three β2 subunits ($n = 5$). n corresponds to the number of independent experiments, each from different cell patches (see Table 1). Solid lines represent the fitted curves. For open, the curve was obtained by linear regression. For bursts, the exponential function parameters were obtained from the linear regression of the ln(τ_{burst}) vs number of β2 subunits (inset). **b** Amplitude histograms for α7 and $(\alpha7)_2(\beta2)_3$ constructed with opening events longer than 0.3 ms

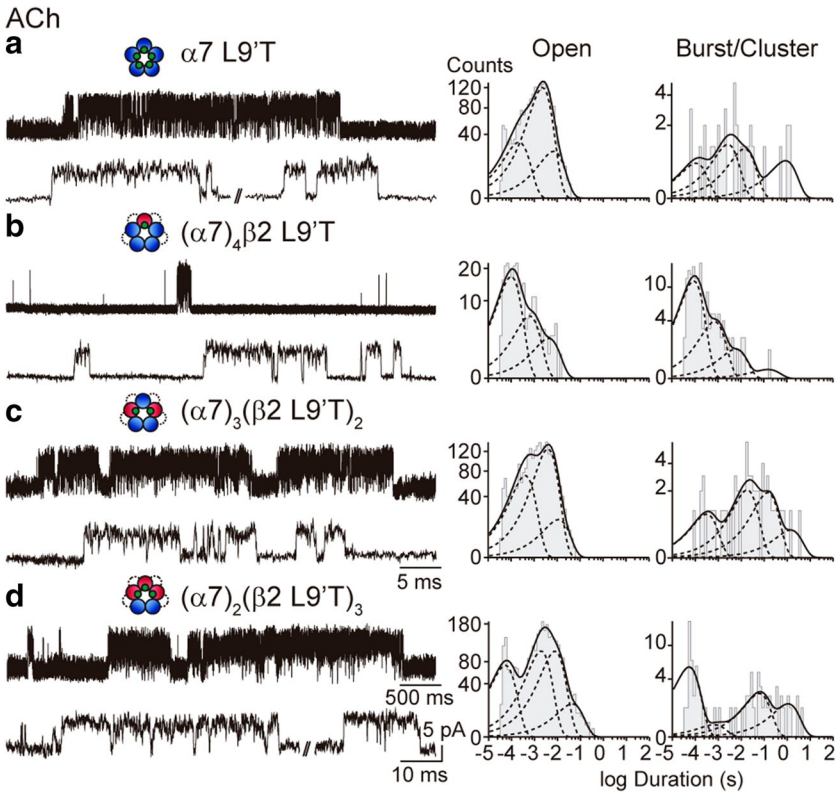

Fig. 6 Single-channel recordings from α7β2 concatemeric receptors containing β2 subunits carrying the L9′T mutation in the TM2 segment. Left: typical traces from single-channel recordings in the continuous presence of 1 mM ACh are shown at two different time scales. For comparison, single-channel activity of α7L9′T is also shown (**a**). The recordings show the longest duration clusters detected. Right: representative duration histograms are shown. Channel openings are shown as upward deflections. Membrane potential: − 70 mV. Filter: 9 kHz

In the presence of 100 μM ACh and 1 μM PNU-120596 (type II PAM), the typical long openings and clusters detected in α7 are also observed for $(\alpha7)_4\beta_2$, $(\alpha7)_3(\beta2)_2$ and $(\alpha7)_2(\beta2)_3$ (Fig. 7a, Table 1). As determined from Table 1, there are no statistically significant differences in the mean open and cluster durations with respect to those of α7 ($p > 0.05$, Fig. 7b, Table 1). Also, macroscopic current recordings in oocytes show no differences in EC_{50} values for

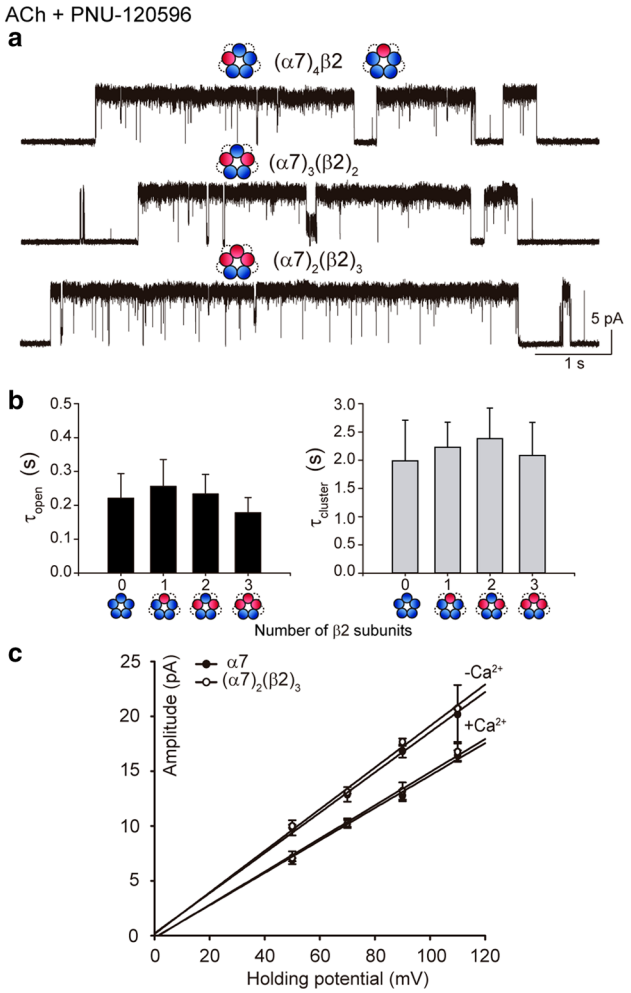

Fig. 7 Potentiation of concatemeric α7β2 receptors by PNU-120596. **a** Single-channel traces of recordings in the continuous presence of 100 μM ACh + 1 μM PNU-120596. Channel openings are shown as upward deflections. Membrane potential: − 70 mV. Filter: 3 kHz. **b** Mean open (τ_{open}) and cluster ($\tau_{cluster}$) durations in presence of PNU-120596. Data are plotted as mean ± SD for zero β2 ($n = 4$), one β2 ($n = 5$), two β2 ($n = 5$) and three β2 subunits ($n = 4$). n corresponds to the number of independent experiments, each from different cell patches (see Table 1). τ_{open} and $\tau_{cluster}$ for β2-containing concatemers in presence of PNU-120596 compared with homomeric α7 do not show significance differences ($p > 0.05$ by two-tailed Student's t test). **c** Curves showing the relationship between the single-channel current amplitude and the holding potential for α7 and $(\alpha7)_2(\beta2)_3$ potentiated by PNU-120596 in the absence or presence of 1.8 mM Ca^{2+} in the pipette solution. Non-statistically significant differences in amplitude at each holding potential are detected between α7 and $(\alpha7)_2(\beta2)_3$ for each condition (two-tailed Student's t test, $p > 0.05$, $n = 3$ independent experiments from different cell patches for each condition)

PNU-120596 between α7 and heteromeric receptors activated by the agonist (Fig. 3b, Table 2). Thus, we conclude that PNU-120596 does not select between homomeric and heteromeric receptors. For all pentameric arrangements, the mean channel amplitude is similar to that of α7 (9.87 ± 0.20, 10.21 ± 0.72, and 10.20 ± 0.26 pA for receptors with one, two or three β2 subunits, respectively, $p > 0.05$, $n = 4$ for each condition).

For α7, single channel activity in the presence of ACh and 2 mM 5-HI (type I PAM) appears in bursts composed of successive openings of prolonged duration [29, 36] (Table 1). For the heteromeric receptors, the increase in open and burst durations due to the presence of 5-HI decreases with the number of β2 subunits (Table 1 and Fig. 8a, b). Although $(\alpha7)_3(\beta2)_2$ and $(\alpha7)_2(\beta2)_3$ have longer durations than α7 in the absence of 5-HI, these durations are significantly briefer than those of α7 in the presence of 5-HI [$n = 4$ for each receptor, $p < 0.01$ for $(\alpha7)_3(\beta2)_2$ and $p < 0.001$ for $(\alpha7)_2(\beta2)_3$]. For each pentameric arrangement, normalization of open and burst durations in the presence of 5-HI to its respective control value in the absence of 5-HI reveals decreased potentiation as a function of the number of β2 and no significant potentiation for $(\alpha7)_2(\beta2)_3$ (Fig. 8b, Table 1). In agreement, negligible 5-HI potentiation of $(\alpha7)_3(\beta2)_2$ is observed from macroscopic current recordings in oocytes (Fig. 3c, Table 2).

In the presence of another type I PAM, NS-1738, α7 receptors show prolonged open channel lifetime and mean burst durations respect to the control [36] (Table 1). The degree of NS-1738 potentiation of $(\alpha7)_2(\beta2)_3$ ($n = 5$), measured by the increase in open ($p < 0.01$) and burst duration ($p < 0.001$), is significantly lower than that of α7 ($n = 4$) (Fig. 8c, d, Table 1). Thus, 5-HI and NS-1738 show higher selectivity for α7 than for heteromeric receptors, whereas PNU-120596 leads to potentiated episodes of similar durations between both receptor types.

In the presence of all PAMs, channel amplitude remains constant among all heteromeric receptors. We took advantage of PNU-120596, which by leading to frequent and prolonged openings allows accurate measurement of single-channel amplitude, to determine the conductance from current–voltage relationships. We found no differences in the conductance between α7 and $(\alpha7)_2(\beta2)_3$ in the presence or absence of calcium ($n = 3$ for each receptor and condition). The mean conductance values are: 155.2 ± 7.0 pS for α7 and 159.8 ± 4.4 pS for $(\alpha7)_2(\beta2)_3$ in 1.8 mM Ca^{2+}, and 175.2 ± 5.8 pS for α7 and 184.0 ± 10.7 pS for $(\alpha7)_2(\beta2)_3$, in the absence of Ca^{2+} (Fig. 7c).

Activation of $(\alpha7)_2(\beta2)_3$ by an α7 allosteric agonist

α7 is activated by the allosteric agonist 4BP-TQS probably through an intrasubunit transmembrane cavity [40, 41]. In α7, this agonist elicits prolonged openings (55.4 ± 40 ms, $n = 4$), which are grouped in very long-duration clusters (1834 ± 970 ms, $n = 4$) (Fig. 9). We found that $(\alpha7)_2(\beta2)_3$

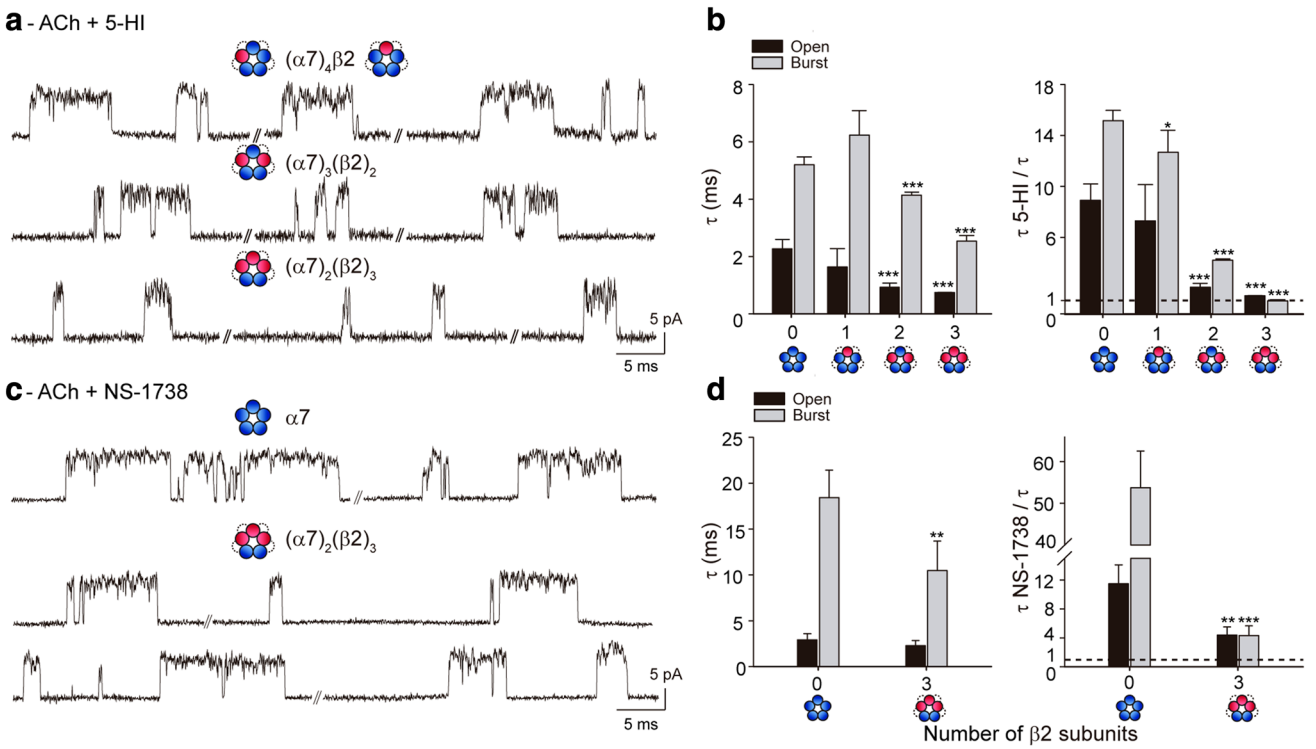

Fig. 8 Potentiation of concatenated α7β2 receptors by 5-HI and NS-1738. Single-channel traces of recordings in the continuous presence of 500 µM ACh and 2 mM 5-HI (**a**) or 10 µM NS-1738 (**c**). Membrane potential: − 70 mV. Filter: 9 kHz. Channel openings are shown as upward deflections. **b**, **d**, Left: mean open (τ_{open}) and burst (τ_{burst}) durations in presence of PAMs. Data are plotted as mean ± SD. For 5-HI $n = 4$ for each condition, for NS-1738 $n = 4$ for α7 and $n = 5$ for $(\alpha7)_2(\beta2)_3$. n corresponds to the number of independent experiments, each from different cell patches (see Table 1). Statistical significance was determined by comparing the durations of β2-containing receptors with respect to α7 in the presence of PAMs, by two-tailed Student's t test ($p < 0.05$*, $p < 0.01$**, $p < 0.001$***). **b**, **d**, Right: mean open and burst durations in the presence of PAMs (shown in **b**, **d**, left) were normalized to the values of their respective control receptors in the absence of PAMs. Statistical significance was determined by comparing the degree of potentiation between β2-containing receptors respect to α7, by two-tailed Student's t test ($p < 0.05$*, $p < 0.01$**, $p < 0.001$***)

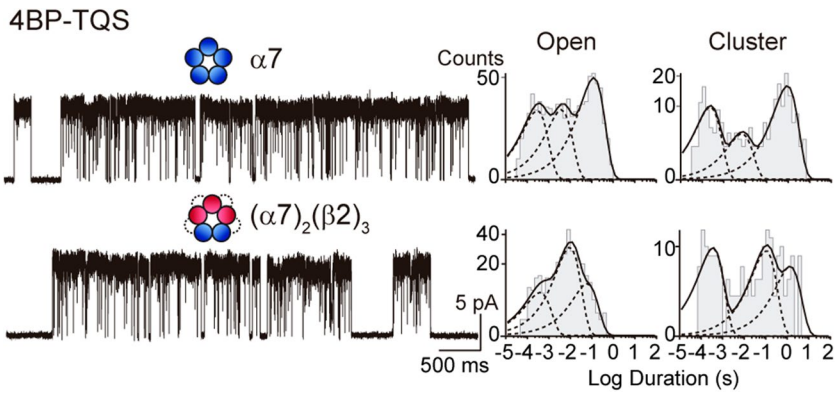

Fig. 9 Allosteric activation of concatenated α7β2 receptors by 4BP-TQS. Left: single-channel traces of α7 and $(\alpha7)_2(\beta2)_3$ from recordings in the continuous presence of 10 µM 4BP-TQS. Right: typical open and cluster duration histograms are shown. Channel openings are shown as upward deflections. Membrane potential: − 70 mV. Filter: 3 kHz

receptors can be also activated by 4BP-TQS. The activation pattern as well as mean open (71.7 ± 38 ms, $n = 6$) and cluster durations (1396 ± 539 ms, $n = 6$) are similar to those of α7 ($p > 0.05$, Fig. 9).

Co-assembly of unlinked α7 and β2 subunits

To confirm that co-assembly of β2 and α7 subunits takes place with unlinked subunits and to establish the stoichiometry of the functional arrangements, we applied the electrical fingerprinting strategy. The strategy is based on the use of an

α7 subunit that contains three arginine substitutions at the intracellular TM3–TM4 loop region (α7LC). Although the receptors are functional as evidenced by macroscopic current recordings, single channels cannot be detected because the amplitude is reduced to undetectable levels [27–31] (Fig. 10a, first trace). Due to the brief duration of α7 openings, the strategy has to be performed in the presence of a modulator that increases open channel lifetime to accurately measure channel amplitude [29, 42]. We here used PNU-120596 since it well potentiates all heteromeric receptors.

When α7 is co-expressed with α7LC, instead of the homogenous amplitude population detected for α7 alone, different amplitude populations can be well distinguished from the histograms (Fig. 10a, second trace). Our previous works show that the different populations report the number of low conductance subunits in each pentameric arrangement [27–29]. Thus, populations of ~ 2, 4, 6, 8 and 10 pA channels correspond to arrangements containing four, three, two, one and zero α7LC subunits, respectively [29–31].

We first used this strategy as an important control of $(\alpha7)_5$. When we co-expressed α7LC with $(\alpha7)_5$, only one amplitude population corresponding to that of wild-type α7 was detected (~ 10 pA), in contrast to the results with α7LC and unlinked α7 ($n = 4$). This result confirms that the α7 concatemeric receptor remains intact and does not yield α7 individual subunits as degradation products (Fig. 10a, third trace).

Although single-channel openings in the presence of ACh and 1 μM PNU-120596 are not detected from cells transfected with α7LC cDNA alone, they are detected when the β2 subunit cDNA is added during transfection (1:8–1:10 subunit ratio). This result indicates that β2 assembles with α7LC. The frequency of the active patches is significantly lower, indicating that the functional expression

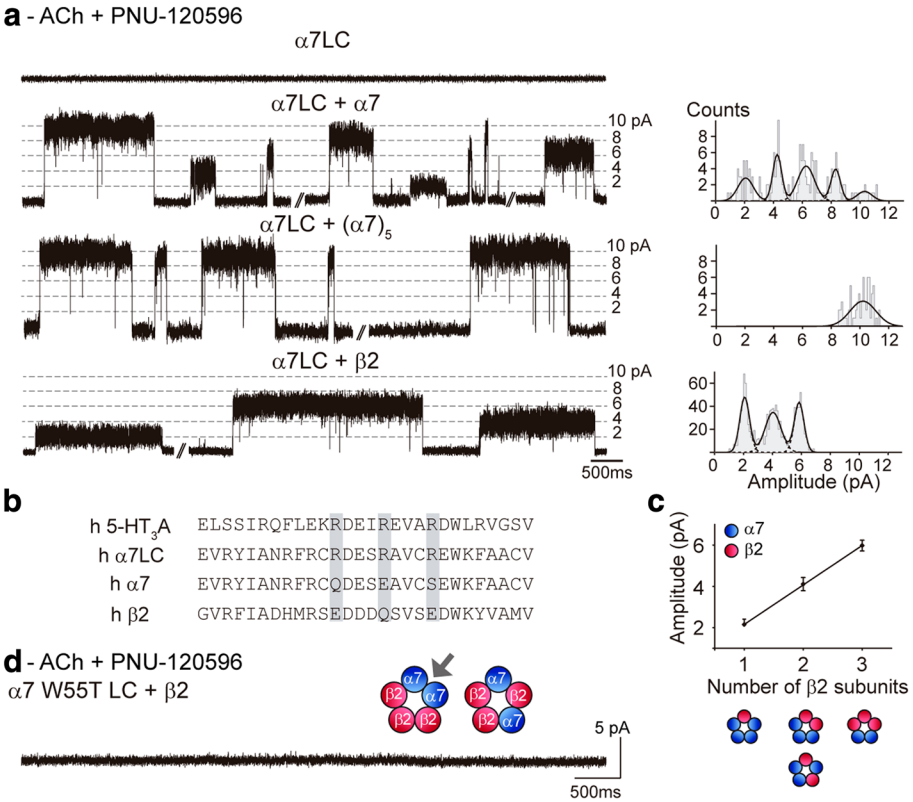

Fig. 10 Electrical fingerprinting strategy. **a** Left: single-channel currents activated by 100 μM ACh + 1 μM PNU-120596 from α7LC, α7LC + α7, α7LC + $(\alpha7)_5$ and α7LC + β2. The traces for the mixed subunits are excerpts from the same recording in the continuous presence of ACh and PNU-120596. Amplitude histograms constructed with events longer than 0.3 ms are shown (right). Membrane potential: − 70 mV. Filter: 3 kHz. Channel openings are shown as upward deflections. **b** Alignment of amino acid sequences of human $5HT_3A$, α7LC, α7 and β2 subunits highlighting the amino acids that determine single-channel conductance. **c** Plot of mean current amplitude against the number of β2 subunits. The fitted slope by least-squares method is 1.91 ± 0.02 pA/β2 subunit. Data are plotted as mean ± SD of $n = 4$ for amplitude classes of 2 pA and 4 pA, and $n = 5$ for the amplitude class of 6 pA. n corresponds to the number of independent experiments, each from different cell patches. **d** Representative single-channel recording in the presence of 100 μM ACh + 1 μM PNU-120596 showing lack of single channel activity from cells expressing α7LC carrying the W55T mutation in loop D [complementary face (−)] and β2 subunits. Membrane potential: − 70 mV. Filter: 3 kHz. Schematic diagrams of $(\alpha7)_2(\beta2)_3$ concatemeric receptor showing possible binding sites at α7/α7 or α7/β2 interfaces are shown. The presence of an α7/α7 interface allows activation (gray arrow)

of heteromeric receptors is lower than that of homomeric receptors. Instead of the five amplitude classes detected for α7 and α7LC, only the three of lower amplitude are detected for α7LC and β2 (Fig. 10a, fourth trace).

Our concatemeric receptors show that β2 subunits do not affect channel amplitude. β2 does not contain the arginine residues at the portal region shown to govern the low conductance of 5-HT_3A and α7LC receptors, instead it contains negatively charged residues as α7 (Fig. 10b). Thus, we infer that the contribution of β2 to α7β2 channel conductance is mainly governed by these portal residues and that each β2 subunit contributes approximately equally (~ 2 pA) to the single-channel conductance (Fig. 10c). In consequence, similarly to the α7:α7LC results (this work and [29]), amplitude classes of ~ 2, 4 and 6 pA would correspond to receptors containing one, two and three β2 subunits, respectively. In line with this, we do not detect the ~ 8 and 10 pA classes, which would correspond to receptors containing four and five β2 subunits, respectively (Fig. 10c).

We conclude that wild-type α7 can assemble with β2 into pentameric arrangements containing one, two or three β2 subunits. As shown for the concatemeric receptors, the open and cluster durations of the amplitude classes in the presence of PNU-120596 are not statistically significantly different from those of α7 ($p > 0.05$, Table 3).

To determine if the β2 subunit contributes to the complementary face of the binding site, we co-expressed β2 with an α7LC subunit containing the W55T mutation at loop D of the complementary face that completely inactivates ACh activation in α7 receptors [27], and recorded single channels in the presence of ACh and 1 μM PNU-120596. The hypothesis is that if activation takes place through the α7/β2 interface, where β2 provides the complementary face of the ACh binding site, single-channel activity should be restored in α7LCW55T/β2 receptors. In a total of 19 patches from three different cell transfections, no channels were detected (Fig. 10d). This result indicates that the α7 complementary face is required for activation and, consequently, that activation of α7β2 occurs mainly through the α7/α7 binding-site interface (Fig. 10d).

Table 3 Mean open and cluster duration of channels corresponding to each amplitude class detected from cells expressing α7LC and β2 in the continuous presence of 100 μM ACh + 1 μM PNU-120596

Amplitude classes (pA)	τ_{open} (ms)	$\tau_{cluster}$ (ms)	*n*
2.15 ± 0.26	108 ± 27	1451 ± 1322	4
4.10 ± 0.32	142 ± 55	1907 ± 752	4
5.97 ± 0.26	179 ± 55	2897 ± 743	5

τ_{open} and $\tau_{cluster}$ correspond to the slowest component of the open and burst or cluster duration histograms, respectively. Values are mean ± SD. *n* corresponds to the number of independent experiments, each from different cell patches. There are not statistically significant differences in τ_{open} and $\tau_{cluster}$ between the distinct amplitude classes and respect to α7, $p > 0.05$ by two-tailed Student's *t* test

Discussion

The discovery of the novel α7β2 receptor inevitably led to key questions regarding its distinct role and location. To find the answers, it is first required to establish the molecular functional differences between α7 and α7β2 receptors that will help distinguish each functional receptor in native cells. However, functional studies using macroscopic current recordings have shown that the impact of the β2 subunit on the pharmacology of the α7β2 receptors, compared to that of α7 homomeric receptors, appears not sufficient to distinguish unequivocally the two receptor subtypes [16, 17, 21, 22]. The fact that α7β2 can assemble into different pentameric arrangements introduces additional complexity. Therefore, there is an urgent need to decipher the features of activation and potentiation contributed by the β2 subunit to the different α7-containing pentameric arrangements.

We here report the first single-channel study of heteromeric α7β2 receptors. By combining single-channel recordings with two different approaches—concatemeric receptor technology and electrical fingerprinting strategy—we reveal the stoichiometry of receptors and the kinetic signature of each pentameric arrangement.

Concatenation of subunits is used as a strategy to express channels with fixed stoichiometry [26]. However, the resulting information should be verified with unlinked subunits to discard that the concatenation allows assembly of subunits that cannot occur in native systems. On the other hand, our established electrical fingerprinting strategy for α7 [27–29, 31], which uses unlinked subunits, can only be applied in the presence of a potentiator that by increasing open duration allows accurate measurement of channel amplitude [29]. Thus, each strategy has proven significant by itself while their combination has provided a complete picture of α7β2 activation and modulation.

We show that α7 co-assembles with one, two or three β2 subunits and that the α7/α7 interface is required for activation [20]. This scenario clearly differs from that in which β2 is combined with α4, where only two receptor stoichiometries, comprising two or three β2 subunits, are functional [43, 44]. It also differs by the fact that in both α4β2 receptor stoichiometries, each β2 subunit contributes to the complementary face of an agonist-binding site and that the additional α4/α4 binding site present in the $(\alpha4)_3(\beta2)_2$ receptor cannot per se drive efficacious activation [24]. Thus, among β2-containing heteromeric receptors, the presence of the α7 subunit provides a unique functional behavior. This discovery opens doors to explore why α7/β2 binding-site interfaces cannot mediate efficacious activation. The conclusion that

only one α7/α7 interface is enough to activate $(\alpha7)_2(\beta2)_3$ receptors is in line with our previous findings showing that only one functional ACh binding site is sufficient for α7 activation [29]. It also agrees with previous results from macroscopic current recordings of α7β2 receptors formed by unlinked subunits [20]. Moreover, the fact that the 8 pA-amplitude class is not detected in recordings from cells co-expressing α7LC and β2 indicates that receptors with four β2 subunits, which should contain one α7/β2 binding-site interface, are not functional.

When compared to α7, heteromeric α7β2 receptors show increased open and burst durations. The open duration increases linearly with the number of β2 subunits whereas the burst duration is more sensitive since it shows an exponential increase. Increased burst duration is probably a consequence of decreased desensitization, indicating that the kinetics of activation and desensitization differs between heteromeric and α7 receptors. This result explains previous observations from macroscopic current recordings showing reduced decay rates for α7β2 [16, 17, 21]. It also explains the variable results regarding its pharmacological properties because in a mixed population of homomeric and different heteromeric arrangements the changes may be too subtle to be resolved at the macroscopic level [22]. The prolonged bursts, never detected in α7, can be used as the signature of the presence of α7β2 receptors. Prolonged activation and reduced desensitization may have an important impact on calcium-dependent intracellular signaling and neuronal excitability.

The two different arrangements of α4β2 receptors—$(\alpha4)_2(\beta2)_3$ and $(\alpha4)_3(\beta2)_2$—show different single-channel amplitude [25]. Unexpectedly, we found that all α7β2 receptors show similar amplitudes to that of α7 and the conductance of $(\alpha7)_2(\beta2)_3$ in the presence of PNU-120596 is not statistically different to that of α7. As described before for α7 [2, 33, 35, 36], α7β2 receptors show a homogenous amplitude population in the presence of PAMs whose mean amplitude is the same as that of the longest duration openings in the absence of PAMs (which can be fully resolved). Therefore, we can infer that β2 contributes mainly to channel kinetics. The determinants governing the different amplitudes of α4β2 arrangements have not been determined to date. However, for α7-containing receptors our electrical fingerprinting strategy shows that portal residues at the intracellular TM3–TM4 domain [45], previously reported as responsible for the low conductance of 5-HT_3A [46, 47] and the high conductance of α7 [29, 31], are the main determinants of channel amplitude. When combined with α7, the contribution of β2 to channel amplitude is mainly governed by these portal residues, and each β2 subunit contributes approximately equally and similarly as α7 to the single-channel amplitude of α7β2 receptors. It is important to note that although the single-channel conductance in high K^+ solution is similar between α7 and $(\alpha7)_2(\beta2)_3$, our results cannot discard differences in calcium selectivity that due to technical reasons could not be determined.

α7 PAMs are emerging as novel therapeutic drugs for neurological and inflammatory disorders. They are promising drugs because they maintain the temporal and spatial characteristics of endogenous activation, are more selective than agonists, and reduce tolerance due to desensitization [2, 7]. PAMs have been classified based on their macroscopic effects on α7, and the determination of their selectivity has been performed under the premise that α7 is a homomeric receptor. It is, therefore, required to establish if they also act at α7β2. We here show that PNU-120596, the prototype type II PAM, which has been typically considered highly selective for α7 [48], cannot select between α7 and α7β2 receptors. Potentiation of α7β2 by this PAM has been suggested in previous macroscopic current studies [17]. Thus, it should be kept in mind that in in vivo situations both receptor types will be potentiated and their kinetic differences will be probably unmasked. On the other hand, the tested type I PAMs appear to be more specific for α7 than for α7β2, and their exposure will make α7 activity prevail over that of α7β2. Indeed, 5-HI potentiation of $(\alpha7)_2(\beta2)_3$ is negligible. Thus, we propose that the characterization of novel PAMs should include their actions at α7β2.

The most plausible explanation for the different actions of PAMs is that they interact at different sites which, in turn, are differently conserved between α7 and β2. To date, there is no structural evidence unequivocally showing the PAM-binding site(s) for α7. One of the key α7 residues for PNU-120596 potentiation or 4BP-TQS allosteric activation, M254, is a leucine in β2, and the α7M254L mutant is insensitive to both compounds [35, 41, 49]. Thus, it could be possible that in α7β2, α7 is the only subunit involved in the actions of these two compounds. NS-1738 (type I) and PNU-120596 (type II) share structural determinants for potentiation [35, 36, 49]. Since the effects of these two PAMs are different on α7 and α7β2, it could be possible that the allosteric mechanism of potentiation differs between homo and heteromeric receptors or between type I and type II PAMs. Thus, our study opens doors to explore new aspects of α7 potentiation and shows that it is possible to selectively potentiate one of the two receptors. This information will help in the design of more specific ligands.

The unique fast kinetics of α7—extremely rapid desensitization and very brief open duration—indicates that this receptor harbors a built-in filtering mechanism against excessive stimulation. Because the incorporation of β2 slows receptor kinetics and reduces desensitization, it is possible that the action of the two receptors occurs at different temporal scales. Our study is focused on deciphering the kinetic differences of the ionotropic responses. However, α7 has been shown to act as a dual ionotropic/metabotropic receptor

[2, 3, 50–52]. Thus, further studies would be required to determine how the metabotropic activity differs between homomeric and heteromeric α7-containing receptors.

The identification of the kinetic signature by which α7β2 can be distinguished from α7 provides tools for the elucidation of its physiological role and functional location in native tissues, which is emerging as a new field of research.

Acknowledgements This work was supported by Grants from Universidad Nacional del Sur (UNS), Agencia Nacional de Promoción Científica y Tecnológica (ANPCYT, PICT 2013 393, PICT 2015 0941), Consejo Nacional de Investigaciones Científicas y Técnicas (CONICET) Argentina and Bill and Melinda Gates Foundation (CB) and Nigel Groome and Brookes University Research Awards (TM and IB). NACHO cDNA and BOSC 23 cells were generously provided by Dr. Sine (Mayo Clinic).

References

1. Thomsen MS, Hansen HH, Timmerman DB, Mikkelsen JD (2010) Cognitive improvement by activation of α7 nicotinic acetylcholine receptors: from animal models to human pathophysiology. Curr Pharm Des 16:323–343. https://doi.org/10.2174/138161210790170094
2. Corradi J, Bouzat C (2016) Understanding the bases of function and modulation of α7 nicotinic receptors: implications for drug discovery. Mol Pharmacol 90:288–299. https://doi.org/10.1124/mol.116.104240
3. Bouzat C, Lasala M, Nielsen BE, Corradi J, del Esandi MC (2017) Molecular function of α7 nicotinic receptors as drug targets. J Physiol. https://doi.org/10.1113/JP275101
4. Dineley KT, Pandya AA, Yakel JL (2015) Nicotinic ACh receptors as therapeutic targets in CNS disorders. Trends Pharmacol Sci 36:96–108. https://doi.org/10.1016/j.tips.2014.12.002
5. Shytle RD, Mori T, Townsend K, Vendrame M, Sun N, Zeng J, Ehrhart J, Silver AA, Sanberg PR, Tan J (2004) Cholinergic modulation of microglial activation by α7 nicotinic receptors. J Neurochem 89:337–343. https://doi.org/10.1046/j.1471-4159.2004.02347.x
6. Changeux JP, Taly A (2008) Nicotinic receptors, allosteric proteins and medicine. Trends Mol Med 14:93–102. https://doi.org/10.1016/j.molmed.2008.01.001
7. Uteshev VV (2014) The therapeutic promise of positive allosteric modulation of nicotinic receptors. Eur J Pharmacol 727:181–185. https://doi.org/10.1016/j.ejphar.2014.01.072
8. Wallace TL, Porter RHP (2011) Targeting the nicotinic alpha7 acetylcholine receptor to enhance cognition in disease. Biochem Pharmacol 82:891–903. https://doi.org/10.1016/j.bcp.2011.06.034
9. Freedman R (2014) α7-nicotinic acetylcholine receptor agonists for cognitive enhancement in schizophrenia. Annu Rev Med 65:245–261. https://doi.org/10.1146/annurev-med-092112-142937
10. Arias HR (2010) Positive and negative modulation of nicotinic receptors, 1st ed. Adv Protein Chem Struct Biol. https://doi.org/10.1016/b978-0-12-381264-3.00005-9
11. Williams DK, Wang J, Papke RL (2011) Positive allosteric modulators as an approach to nicotinic acetylcholine receptor-targeted therapeutics: advantages and limitations. Biochem Pharmacol 82:915–930. https://doi.org/10.1016/j.bcp.2011.05.001
12. Bertrand D, Gopalakrishnan M (2007) Allosteric modulation of nicotinic acetylcholine receptors. Biochem Pharmacol 74:1155–1163. https://doi.org/10.1016/j.bcp.2007.07.011
13. Chatzidaki A, Millar NS (2015) Allosteric modulation of nicotinic acetylcholine receptors. Biochem Pharmacol 97:408–417. https://doi.org/10.1016/j.bcp.2015.07.028
14. Liu Q, Huang Y, Xue F, Simard A, DeChon J, Li G, Zhang J, Lucero L, Wang M, Sierks M, Hu G, Chang Y, Lukas RJ, Wu J (2009) A novel nicotinic acetylcholine receptor subtype in basal forebrain cholinergic neurons with high sensitivity to amyloid peptides. J Neurosci 29:918–929. https://doi.org/10.1523/JNEUROSCI.3952-08.2009
15. Liu Q, Huang Y, Shen J, Steffensen S, Wu J (2012) Functional α7β2 nicotinic acetylcholine receptors expressed in hippocampal interneurons exhibit high sensitivity to pathological level of amyloid β peptides. BMC Neurosci 13:155–166. https://doi.org/10.1186/1471-2202-13-155
16. Moretti M, Zoli M, George AA, Lukas RJ, Pistillo F, Maskos U, Whiteaker P, Gotti C (2014) The novel α7β2-nicotinic acetylcholine receptor subtype is expressed in mouse and human basal forebrain: biochemical and pharmacological characterization. Mol Pharmacol 86:306–317. https://doi.org/10.1124/mol.114.093377
17. Thomsen MS, Zwart R, Ursu D, Jensen MM, Pinborg LH, Gilmour G, Wu J, Sher E, Mikkelsen JD (2015) α7 and β2 nicotinic acetylcholine receptor subunits form heteromeric receptor complexes that are expressed in the human cortex and display distinct pharmacological properties. PLoS One 10:e0130572. https://doi.org/10.1371/journal.pone.0130572
18. Mowrey DD, Liu Q, Bondarenko V, Chen Q, Seyoum E, Xu Y, Wu J, Tang P (2013) Insights into distinct modulation of α7 and α7β2 nicotinic acetylcholine receptors by the volatile anesthetic. J Biol Chem 288:35793–35800. https://doi.org/10.1074/jbc.M113.508333
19. Liu Q, Xie X, Lukas RJ, St John PA, Wu J (2013) A novel nicotinic mechanism underlies β-amyloid-induced neuronal hyperexcitation. J Neurosci 33:7253–7263. https://doi.org/10.1523/JNEUROSCI.3235-12.2013
20. Murray TA, Bertrand D, Papke RL, George AA, Pantoja R, Srinivasan R, Liu Q, Wu J, Whiteaker P, Lester HA, Lukas RJ (2012) α7β2 nicotinic acetylcholine receptors assemble, function, and are activated primarily via their α7–α7 interfaces. Mol Pharmacol 81:175–188. https://doi.org/10.1124/mol.111.074088
21. Zwart R, Strotton M, Ching J, Astles PC, Sher E (2014) Unique pharmacology of heteromeric α7β2 nicotinic acetylcholine receptors expressed in *Xenopus laevis* oocytes. Eur J Pharmacol 726:77–86. https://doi.org/10.1016/j.ejphar.2014.01.031
22. Wu J, Liu Q, Tang P, Mikkelsen JD, Shen J, Whiteaker P, Yakel JL (2016) Heteromeric α7β2 nicotinic acetylcholine receptors in the brain. Trends Pharmacol Sci 37:562–574. https://doi.org/10.1016/j.tips.2016.03.005
23. Carbone AL, Moroni M, Groot-Kormelink PJ, Bermudez I (2009) Pentameric concatenated (α4)2 (β2)3 and (α4)3(β2)2 nicotinic acetylcholine receptors: subunit arrangement determines functional expression. Br J Pharmacol 156:970–981. https://doi.org/10.1111/j.1476-5381.2008.00104.x
24. Mazzaferro S, Benallegue N, Carbone A, Gasparri F, Vijayan R, Biggin PC, Moroni M, Bermudez I (2011) Additional Acetylcholine (ACh) binding site at α4/α4 interface of (α4β2)2α4 nicotinic receptor influences agonist sensitivity. J Biol Chem 286:31043–31054. https://doi.org/10.1074/jbc.M111.262014
25. Mazzaferro S, Bermudez I, Sine SM, Stephenson FA (2017) α4β2 nicotinic acetylcholine receptors; relationships between subunit stoichiometry and function at the single channel level. J Biol Chem 292:2729–2740. https://doi.org/10.1074/jbc.M116.764183
26. Ericksen SS, Boileau AJ (2007) Tandem couture: Cys-loop receptor concatamer insights and caveats. Mol Neurobiol 35:113–127. https://doi.org/10.1007/BF02700627
27. Rayes D, De Rosa MJ, Sine SM, Bouzat C (2009) Number and locations of agonist binding sites required to activate homomeric

Cys-loop receptors. J Neurosci 29:6022–6032. https://doi.org/10.1523/JNEUROSCI.0627-09.2009
28. Andersen N, Corradi J, Bartos M, Sine SM, Bouzat C (2011) Functional relationships between agonist binding sites and coupling regions of homomeric Cys-loop receptors. J Neurosci 31:3662–3669. https://doi.org/10.1523/JNEUROSCI.5940-10.2011
29. Andersen N, Corradi J, Sine SM, Bouzat C (2013) Stoichiometry for activation of neuronal α7 nicotinic receptors. Proc Natl Acad Sci USA 110:20819–20824. https://doi.org/10.1073/pnas.1315775110
30. daCosta CJB, Free CR, Sine SM (2015) Stoichiometry for α-bungarotoxin block of α7 acetylcholine receptors. Nat Commun 6:8057. https://doi.org/10.1038/ncomms9057
31. daCosta CJB, Sine SM (2013) Stoichiometry for drug potentiation of a pentameric ion channel. Proc Natl Acad Sci USA 110:6595–6600. https://doi.org/10.1073/pnas.1301909110
32. Benallegue N, Mazzaferro S, Alcaino C, Bermudez I (2013) The additional ACh binding site at the α4(+)/α4(−) interface of the (α4β2)2α4 nicotinic ACh receptor contributes to desensitization. Br J Pharmacol 170:304–316. https://doi.org/10.1111/bph.12268
33. Bouzat C, Bartos M, Corradi J, Sine SM (2008) The interface between extracellular and transmembrane domains of homomeric Cys-loop receptors governs open-channel lifetime and rate of desensitization. J Neurosci 28:7808–7819. https://doi.org/10.1523/JNEUROSCI.0448-08.2008
34. Bouzat C, Bren N, Sine SM (1994) Structural basis of the different gating kinetics of fetal and adult acetylcholine receptors. Neuron 13:1395–1402. https://doi.org/10.1016/0896-6273(94)90424-3
35. DaCosta CJB, Free CR, Corradi J, Bouzat C, Sine SM (2011) Single-channel and structural foundations of neuronal α7 acetylcholine receptor potentiation. J Neurosci 31:13870–13879. https://doi.org/10.1523/JNEUROSCI.2652-11.2011
36. Andersen ND, Nielsen BE, Corradi J, Tolosa MF, Feuerbach D, Arias HR, Bouzat C (2016) Exploring the positive allosteric modulation of human α7 nicotinic receptors from a single-channel perspective. Neuropharmacology 107:189–200. https://doi.org/10.1016/j.neuropharm.2016.02.032
37. Pałczynska MM, Jindrichova M, Gibb AJ, Millar NS (2012) Activation of α7 nicotinic receptors by orthosteric and allosteric agonists: influence on single-channel kinetics and conductance. Mol Pharmacol 82:910–917. https://doi.org/10.1124/mol.112.080259
38. Aryal P, Sansom MSP, Tucker SJ (2015) Hydrophobic gating in ion channels. J Mol Biol 427:121–130. https://doi.org/10.1016/j.jmb.2014.07.030
39. Revah F, Bertrand D, Galzi JL, Devillers-Thiéry A, Mulle C, Hussy N, Bertrand S, Ballivet M, Changeux JP (1991) Mutations in the channel domain alter desensitization of a neuronal nicotinic receptor. Nature 353:846–849. https://doi.org/10.1038/353846a0
40. Gill JK, Chatzidaki A, Ursu D, Sher E, Millar NS (2013) Contrasting properties of α7-selective orthosteric and allosteric agonists examined on native nicotinic acetylcholine receptors. PLoS One 8:e55047. https://doi.org/10.1371/journal.pone.0055047
41. Gill JK, Savolainen M, Young GT, Zwart R, Sher E, Millar NS (2011) Agonist activation of alpha7 nicotinic acetylcholine receptors via an allosteric transmembrane site. Proc Natl Acad Sci USA 108:5867–5872. https://doi.org/10.1073/pnas.1017975108
42. Bouzat C, Sine SM (2017) Nicotinic acetylcholine receptors at the single-channel level. Br J Pharmacol. https://doi.org/10.1111/bph.13770
43. Nelson ME, Kuryatov A, Choi CH, Zhou Y, Lindstrom J (2003) Alternate stoichiometries of alpha4beta2 nicotinic acetylcholine receptors. Mol Pharmacol 63:332–341. https://doi.org/10.1124/mol.63.2.332
44. Moroni M, Vijayan R, Carbone A, Zwart R, Biggin PC, Bermudez I (2008) Non-agonist-binding subunit interfaces confer distinct functional signatures to the alternate stoichiometries of the α4β2 nicotinic receptor: an α4–α4 interface is required for Zn^{2+} potentiation. J Neurosci 28:6884–6894. https://doi.org/10.1523/JNEUROSCI.1228-08.2008
45. Hassaine G, Deluz C, Grasso L, Wyss R, Tol MB, Hovius R, Graff A, Stahlberg H, Tomizaki T, Desmyter A, Moreau C, Li X-D, Poitevin F, Vogel H, Nury H (2014) X-ray structure of the mouse serotonin 5-HT3 receptor. Nature 512:276–281. https://doi.org/10.1038/nature13552
46. Kelley SP, Dunlop JI, Kirkness EF, Lambert JJ, Peters JA (2003) A cytoplasmic region determines single-channel conductance in 5-HT3 receptors. Nature 424:321–324. https://doi.org/10.1038/nature01788
47. Corradi J, Gumilar F, Bouzat C (2009) Single-channel kinetic analysis for activation and desensitization of homomeric 5-HT3A receptors. Biophys J 97:1335–1345. https://doi.org/10.1016/j.bpj.2009.06.018
48. Hurst RS, Hajos M, Raggenbass M, Wall TM, Higdon NR, Lawson JA, Rutherford-Root KL, Berkenpas MB, Hoffmann WE, Piotrowski DW, Groppi VE, Allaman G, Ogier R, Bertrand S, Bertrand D, Arneric SP (2005) A novel positive allosteric modulator of the α7 neuronal nicotinic acetylcholine receptor. In vitro and in vivo characterization. J Neurosci 25:4396–4405. https://doi.org/10.1523/JNEUROSCI.5269-04.2005
49. Young GT, Zwart R, Walker AS, Sher E, Millar NS (2008) Potentiation of α7 nicotinic acetylcholine receptors via an allosteric transmembrane site. Proc Natl Acad Sci USA 105:14686–14691. https://doi.org/10.1073/pnas.0804372105
50. Paulo JA, Brucker WJ, Hawrot E (2009) Proteomic analysis of an α7 nicotinic acetylcholine receptor interactome. J Proteome Res 8:1849–1858. https://doi.org/10.1021/pr800731z
51. Nordman JC, Kabbani N (2012) An interaction between α7 nicotinic receptors and a G-protein pathway complex regulates neurite growth in neural cells. J Cell Sci 125:5502–5513. https://doi.org/10.1242/jcs.110379
52. Kabbani N, Nordman JC, Corgiat BA, Veltri DP, Shehu A, Seymour VA, Adams DJ (2013) Are nicotinic acetylcholine receptors coupled to G proteins? Bioessays 35:1025–1034. https://doi.org/10.1002/bies.201300082